

Supplementary Information

**Metallic nanoparticles immobilized in magnetic metal-organic
frameworks: preparation and application as highly active,
magnetically isolable and reusable catalysts**

Hai-juan Zhang ^a, Sheng-da Qi ^a, Xiao-ying Niu ^a, Jing Hu ^a, Cui-ling Ren ^a, Hong-li Chen ^a, Xing-guo Chen ^{a, b,*}

^a State Key Laboratory of Applied Organic Chemistry, College of Chemistry and Chemical Engineering, Lanzhou University, Lanzhou, Gansu 730000, China;

^b Key Laboratory of Nonferrous Metal Chemistry and Resources Utilization of Gansu Province, Lanzhou University, Lanzhou, Gansu 730000, China

* Corresponding author

E-mail address: chenxg@lzu.edu.cn

Tel: 86-931-8912763

Fax: 86-931-8912582

Table S1. Elemental and ICP analyses for the samples.

Sample	Found (%)
Fe ₃ O ₄ @Pt/MIL-100 (Fe) (15 cycles)	C, 9.15; H, 1.27; Fe, 45.49; Pt, 4.26
Fe ₃ O ₄ @Pt/MIL-100 (Fe) (20 cycles)	C, 10.06; H, 1.39; Fe, 43.99; Pt, 4.29
Fe ₃ O ₄ @Pt/MIL-100 (Fe) (30 cycles)	C, 14.02; H, 1.76; Fe, 39.22; Pt, 4.07
Fe ₃ O ₄ @Pt/MIL-100 (Fe) (40 cycles)	C, 15.61; H, 2.01; Fe, 36.38; Pt, 3.93
Fe ₃ O ₄ @Pt/MIL-100 (Fe) (60 cycles)	C, 19.73; H, 2.41; Fe, 30.02; Pt, 3.67

Table S2. Reduction of various nitrobenzenes using Fe₃O₄@Au/MIL-100 (Fe) catalyst ^a.

Entry	Compound	Structure	Time/min	Conversion (%)	TOF (h ⁻¹)
1	<i>o</i> -Nitrophenol		15	93.2	144
2	<i>m</i> -Nitrophenol		6	96.8	374
3	<i>p</i> -Nitrophenol		10	96.2	223
4	2,4-Dinitrophenol		44	96.2	51
5	<i>o</i> -Nitroaniline		10.5	95.2	210
6	<i>m</i> -Nitroaniline		9	96.5	249
7	<i>p</i> -Nitroaniline		20.5	96.6	109
8	4-Methyl-3-nitroaniline		16.5	90.1	127
9	4-Methyl-2-nitroaniline		39	96.2	57
10	<i>p</i> -Nitrophenylhydrazine		10.5	93.9	208

^a Reaction condition: 25 μL of 10 mM nitrobenzene, 25 μL of 1.0 mg/mL catalyst, and 200 μL of 100 mM fresh NaBH₄.

Table S3. Reduction of various nitrobenzenes using Fe₃O₄@Pd/MIL-100 (Fe) catalyst ^a.

Entry	Compound	Structure	Time/min	Conversion	TOF (h ⁻¹)
1	<i>o</i> -Nitrophenol		2	94.6	778
2	<i>m</i> -Nitrophenol		1	94.2	1550
3	<i>p</i> -Nitrophenol		1.2	95.2	1343
4	2,4-Dinitrophenol		13.5	97.3	119
5	<i>o</i> -Nitroaniline		2.5	97.3	641
6	<i>m</i> -Nitroaniline		2	93.4	768
7	<i>p</i> -Nitroaniline		4	97.6	401
8	4-Methyl-3-nitroaniline		6	93.5	256
9	4-Methyl-2-nitroaniline		9	92.6	169
10	<i>p</i> -Nitrophenylhydrazine		6	96.4	264

^a Reaction condition: 25 μL of 10 mM nitrobenzene, 25 μL of 1.0 mg/mL catalyst, and 200 μL of 100 mM NaBH₄. fresh

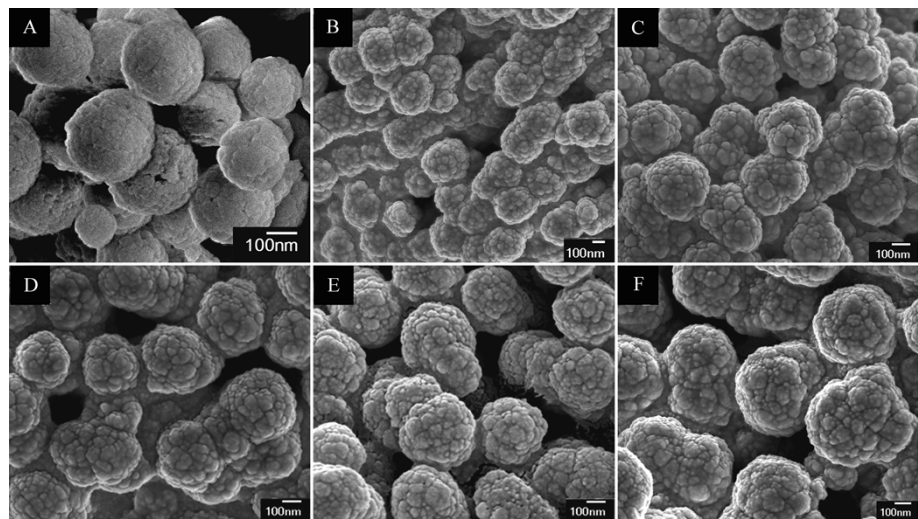


Figure S1. SEM images of (A) Fe_3O_4 and $\text{Fe}_3\text{O}_4@\text{MIL-100}(\text{Fe})$ core-shell microspheres after (B) 15, (C) 20, (D) 30, (E) 40, and (F) 60 assembly cycles.

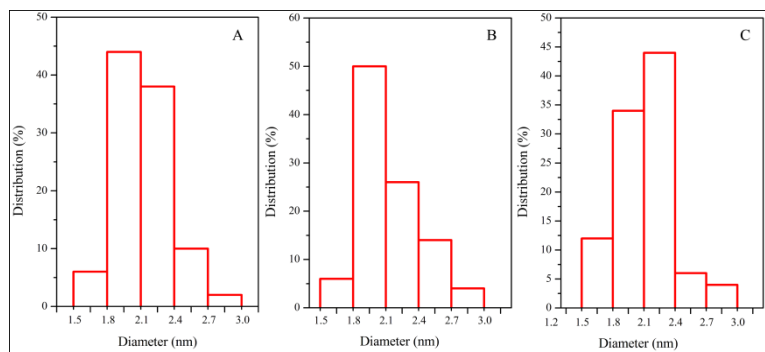


Figure S2. Size distribution of (A) Au NPs, (B) Pt NPs and (C) Pd NPs.

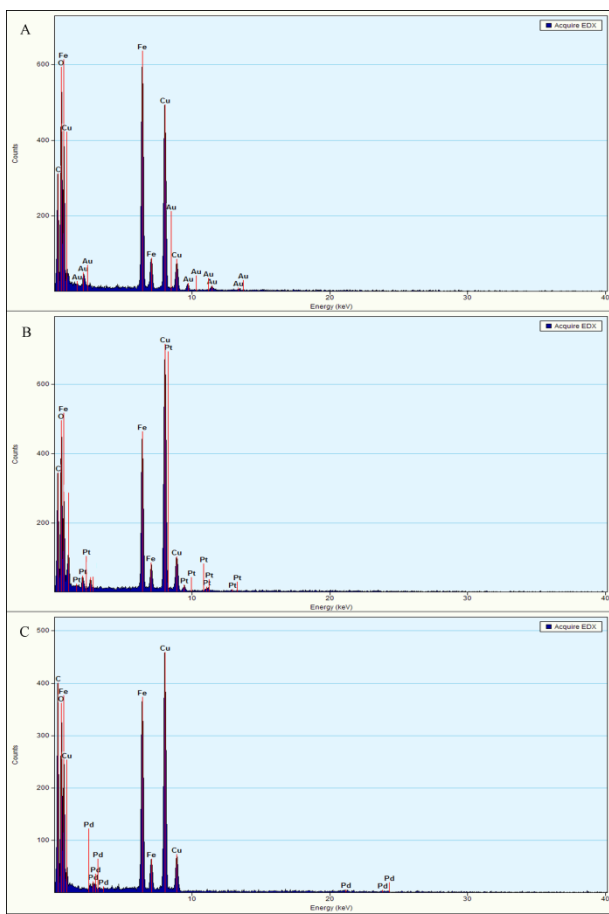


Figure S3. EDX spectra of the Fe₃O₄@MIL-100 (Fe) microspheres with 20 assembly cycles after embedded with (A) Au, (B) Pt, (C) Pd NPs. The copper signal originates from Cu grid.

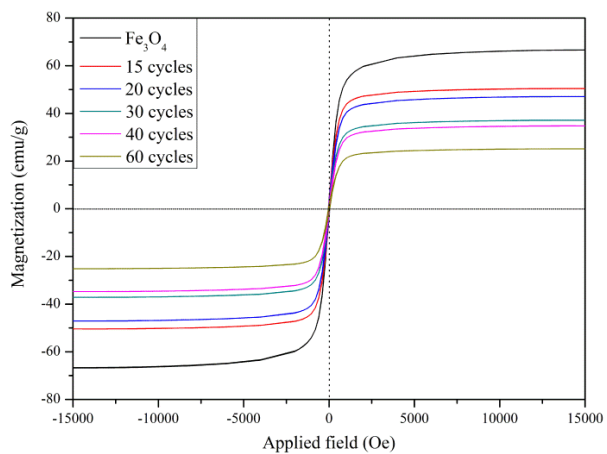


Figure S4. Room-temperature magnetic hysteresis loops of Fe_3O_4 and $\text{Fe}_3\text{O}_4@\text{MIL-100}$ (Fe) core-shell microspheres after 15, 20, 30, 40, and 60 assembly cycles.

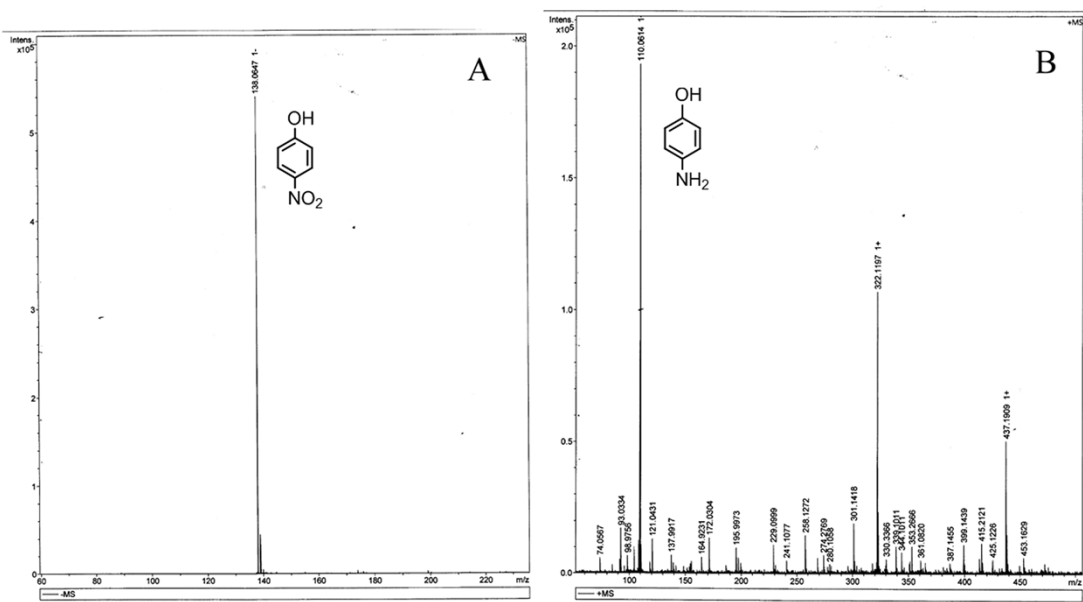


Figure S5. The gas chromatography-mass spectra of (A) *p*-nitrophenol and (B) the product of reduction reaction of *p*-nitrophenol.

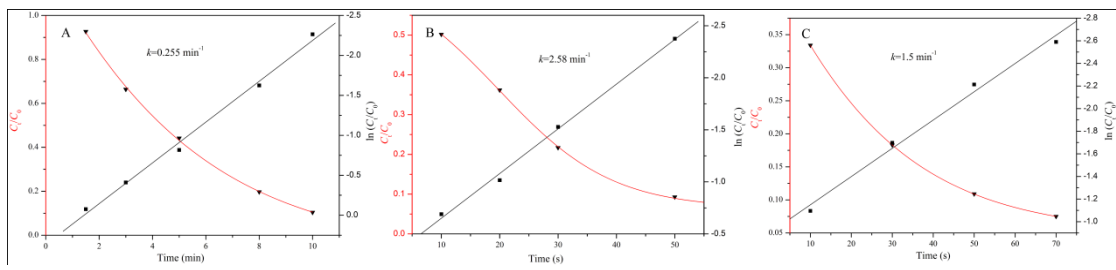


Figure S6. The C_t/C_0 (red) and $\ln(C_t/C_0)$ (black) *versus* the reaction time for the reduction of *p*-nitrophenol by NaBH_4 in presence of 25 μg catalyst: (A) $\text{Fe}_3\text{O}_4@\text{Au}/\text{MIL}-100$ (Fe), (B) $\text{Fe}_3\text{O}_4@\text{Pt}/\text{MIL}-100$ (Fe), and (C) $\text{Fe}_3\text{O}_4@\text{Pd}/\text{MIL}-100$ (Fe) with 20 assembly cycles. Conditions: $[p\text{-nitrophenol}] = 0.083 \text{ mM}$; $[\text{NaBH}_4] = 6.67 \text{ mM}$, 25 $^\circ\text{C}$.

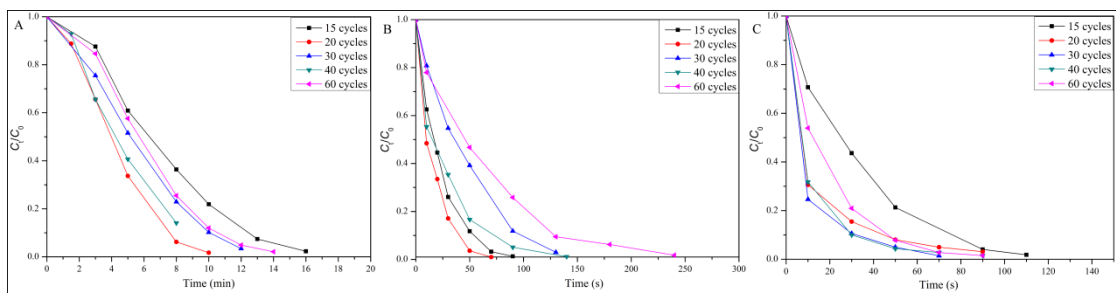


Figure. C_t/C_0 versus reaction time for the reduction of -nitrophenol with the catalysts: (A) $\text{Fe}_3\text{O}_4@\text{Au}/\text{MIL}-100$ (Fe), (B) $\text{Fe}_3\text{O}_4@\text{Pt}/\text{MIL}-100$ (Fe), and (C) $\text{Fe}_3\text{O}_4@\text{Pd}/\text{MIL}-100$ (Fe) after different assembly cycles.

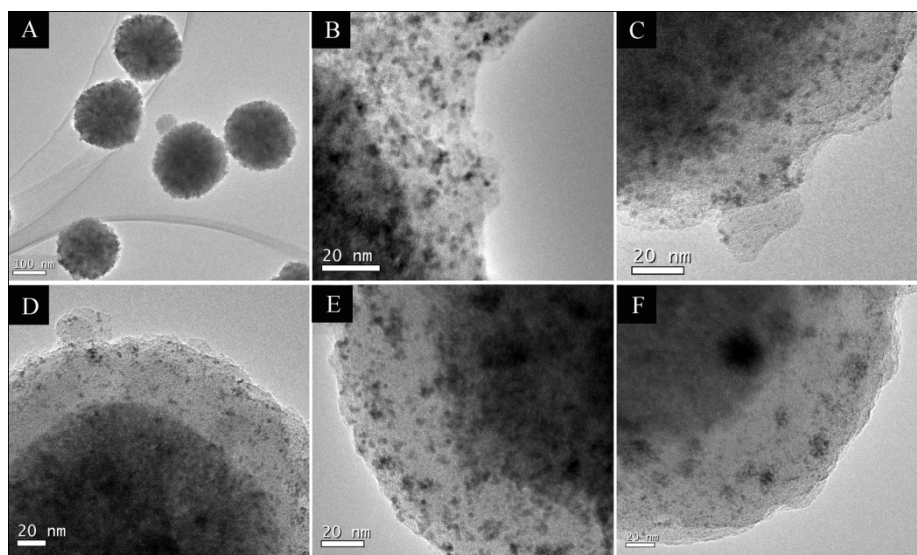


Figure S8. TEM images of individual (A) Fe_3O_4 and $\text{Fe}_3\text{O}_4@\text{Pt}/\text{MIL}-100$ (Fe) core-shell nanospheres after (B) 15, (C) 20, (D) 30, (E) 40, and (F) 60 assembly cycles.

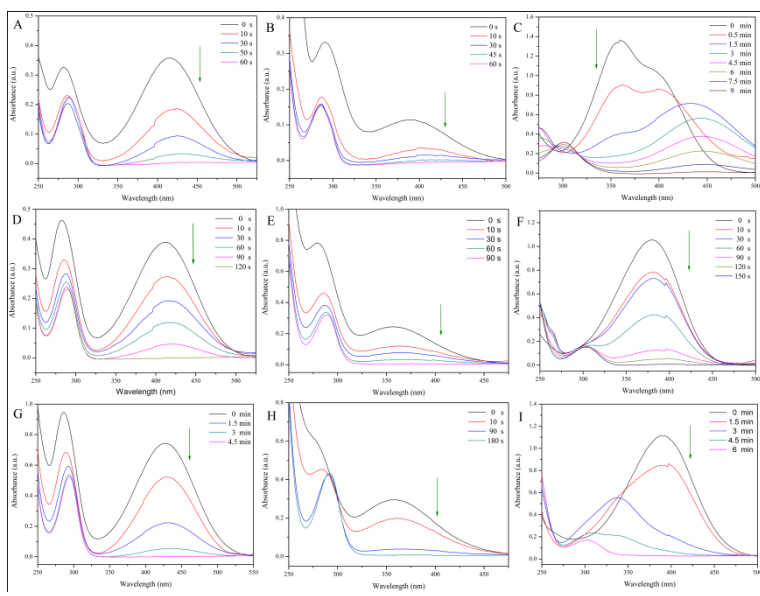


Figure S9. The UV-Vis absorption spectra change for the reduction process of (A) *o*-nitrophenol, (B) *m*-nitrophenol, (C) 2,4-dinitrophenol, (D) *o*-nitroaniline, (E) *m*-nitroaniline, (F) *p*-nitroaniline, (G) 4-Methyl-2-nitroaniline, (H) 4-Methyl-3-nitroaniline and (I) *p*-Nitrophenylhydrazine by NaBH_4 in the presence of $\text{Fe}_3\text{O}_4@\text{Pt}/\text{MIL-100}(\text{Fe})$ catalyst.

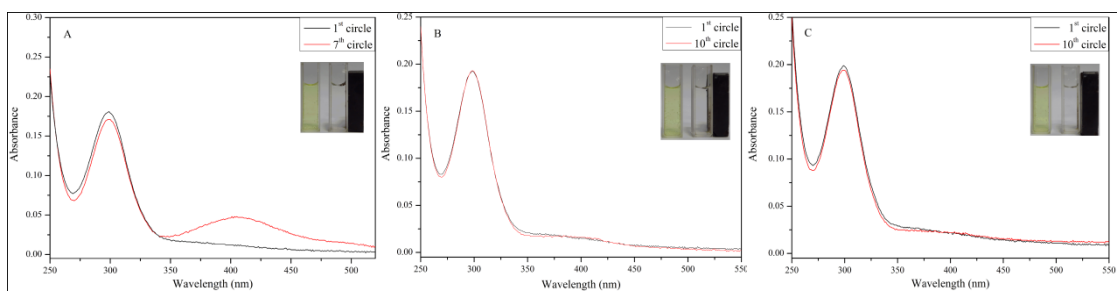


Figure S10. UV-Vis spectra of 4p-nitrophenol reduction with the as-prepared catalysts in different cycles: (A) $\text{Fe}_3\text{O}_4@\text{Au}/\text{MIL}-100$ (Fe), (B) $\text{Fe}_3\text{O}_4@\text{Pt}/\text{MIL}-100$ (Fe), and (C) $\text{Fe}_3\text{O}_4@\text{Pd}/\text{MIL}-100$ (Fe) with 20 assembly cycles. Inset showed the digital image of reaction solution after reaction for different cycles.

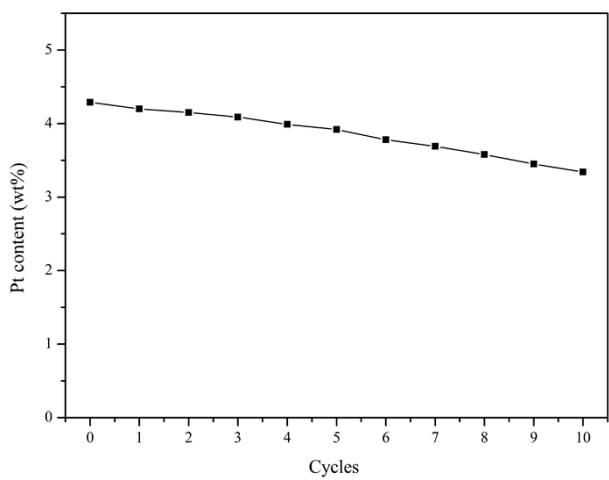


Figure S11. Changes of Pt content after each cycle.